

INTERNATIONAL SOCIETY FOR SOIL MECHANICS AND GEOTECHNICAL ENGINEERING



This paper was downloaded from the Online Library of the International Society for Soil Mechanics and Geotechnical Engineering (ISSMGE). The library is available here:

<https://www.issmge.org/publications/online-library>

This is an open-access database that archives thousands of papers published under the Auspices of the ISSMGE and maintained by the Innovation and Development Committee of ISSMGE.

Centrifuge model tests on circular and rectangular tunnels subjected to large earthquake-induced deformation

T. Yamada, H. Nagatani & H. Igarashi
Kajima Technical Research Institute, Chofu-shi, Tokyo, Japan

A. Takahashi
Tokyo Institute of Technology, Meguro-ku, Tokyo, Japan

ABSTRACT: Evaluation of seismic performance of tunnels in the transverse direction is becoming increasingly important, since many tunnels with a large cross-sectional areas or a complex cross-sectional profile have been constructed in recent years and they need to be designed to with consideration of large earthquakes. However, there are many cases where it is difficult to validate design method accuracy, since methods for analyzing the behavior of such tunnels during large earthquakes have not yet been established. In order to solve this problem and to understand the response of such tunnels subjected to cyclic large shear deformation, the authors conducted centrifuge model tests on three types of tunnel in large soil deformation using an active type shear box: circular tunnel, rectangular tunnel with center columns, and combination of these (triple-faced tunnel consisting of two circular tunnels and a rectangular tunnel). Test results reveal that bending moment and axial force distributions of the circular and rectangular tunnels in the triple-faced tunnel are similar to those in single circular and rectangular tunnels, respectively. However magnitudes of the maximum bending moment in the triple-faced rectangular tunnel differed from that in single rectangular tunnel, since the ground adjacent to the tunnels showed different displacement due to complicated tunnel—soil—tunnel interaction.

1 INTRODUCTION

In order to utilize limited urban underground spaces, construction of new type tunnels (e.g. large cross-section tunnels, specially-shaped tunnels, and multi-faced tunnel) is increasing in Japan in recent years. Such tunnels need seismic evaluation in the transverse direction as well as the longitudinal direction. Since the 1995 Kobe Earthquake, there is a growing awareness that the seismic design of underground structures against large earthquakes is important.

Although a framed structure analysis subjected to ground deformation through soil—structure interaction springs in pseudo-static condition and a dynamic response analysis are generally used for the seismic design of tunnels for the transverse direction, accuracy of analysis results is often controversial when they are applied to designing large cross-section tunnels and specially-shaped tunnels. In order to understand soil—tunnel interactions for large cross-section and specially-shaped tunnels, the authors performed centrifuge model tests in which cyclic shear deformation was statically applied to the model ground (consisting of a tunnel model and surrounding sand) placed in an active type shear box. Three different types of model tunnel were prepared: circular tunnel, rectangular tunnel, and combination of these two (triple-faced tunnel).

2 OUTLINE OF CENTRIFUGE MODEL TESTS

2.1 Loading apparatus

The active type shear box used in the tests is shown in Figure 1. The shear box consisted of thirteen-stacked 24mm-thick alumite coated duralumin laminae supported by roller bearings, which are mounted in grooves on each laminae. Three hydraulic actuators are connected with the three laminae, Nos.5, 9 and 13, directly, and lateral forces are transmitted to

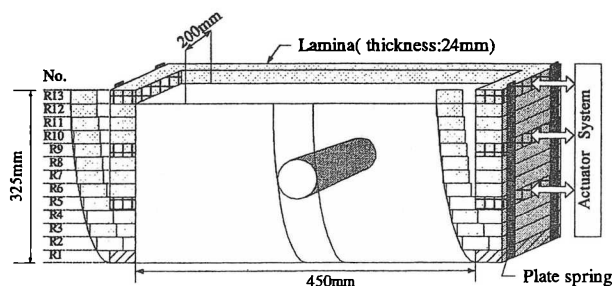


Figure 1. View of the shear box.

No.	CASE1	CASE2	CASE3
	Single Circular Tunnel	Single Rectangular Tunnel	Triple-faced Tunnel
Test Model			
Measurement Items	Sectional Force : Strain Gauge (16*2=32 point, Fig. 3) Settlement of ground : Laser Displacement Meter (3 point) Horizontal Displacement on ground surface : CCD Camera and Targets (35 point) Horizontal Displacement of lamina : Potentiometer (R2- R13 : 12 point)	Sectional Force : Strain Gauge (23*2=46 point, Fig. 3) Settlement of ground : Laser Displacement Meter (3 point) Horizontal Displacement on ground surface : CCD Camera and Targets (12 point) Horizontal Displacement of lamina : Potentiometer (R2- R13 : 12 point) Horizontal Relative Displacement between top and bottom slabs: Non-Contact Displacement Sensor (1 point)	Sectional Force : Strain Gauge (29*2=58 point, Fig. 3) Settlement of ground : Laser Displacement Meter (3 point) Horizontal Displacement on ground surface : CCD Camera and Targets (12 point) Horizontal Displacement of lamina : Potentiometer (R2- R13 : 12 point) Horizontal Relative Displacement between top and bottom slabs for rectangular tunnel: Non-Contact Displacement Sensor (1 point)
Centrifugal Acceleration : 50 G **: Thick lines indicate the measurement positions by strain gauges. Dimensions in this figure indicate scale of the models. Dimensions in parentheses indicate the prototype scale.			

Figure 2. Test cases.

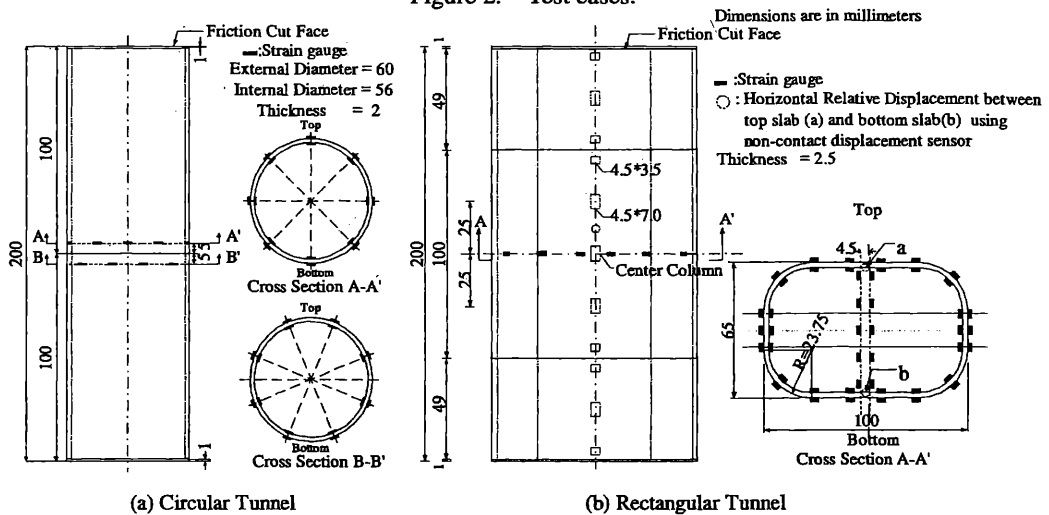


Figure 3. Outline of tunnel models and measurements.

the other laminae through four linked sets of plate springs.

2.2 Model ground

The Toyoura sand (specific gravity: 2.64, maximum void ratio: 0.978, minimum void ratio: 0.605) was used for the model ground. The model ground was prepared by air pluviation to achieve a relative density of 90%. The tunnel model was installed in position during the placement of the sand. In order to take into consideration the shape and mechanical properties (e.g. modulus of elasticity) of actual tunnels, dimensions of the aluminum-made models for the circular tunnel and rectangular tunnel with center columns were determined. Model setups for three test cases are shown in Figure 2, and the details of the tunnel models and the locations of measurement point are illustrated in Figure 3. The measurement items included the strains for both sides of the tunnel lining and center columns (which were used for

calculating the axial forces and bending moments) and the relative horizontal displacement between the top and bottom slabs of the rectangular tunnel (which were measured by gap sensor). At the both ends of the tunnel models, measures were taken to reduce friction between the tunnels and the shear box.

2.3 Test conditions

Having prepared the model, the model was put in a centrifugal acceleration field of 50 G. After outputs of all the sensors were stabilized at 50G, eight-step cyclic triangularly-shaped horizontal displacements were applied to the lamina box. In each cycle, 200-second cycle sinusoidal motions were applied to the lamina box, where the peak values of the applied waves were increased after applying three cycles, up to 6.4mm at the top lamina as summarized in Table 1.

Table 1. Loading steps (displacements). (mm)

Step	1	2	3	4	5	6	7	8
Lamina No.13	0.050	0.100	0.200	0.400	0.800	1.600	3.200	6.400
Lamina No.9	0.033	0.067	0.133	0.267	0.533	1.067	2.133	4.267
Lamina No.5	0.017	0.033	0.067	0.133	0.267	0.533	1.067	2.133
Average Shear Strain (%)	0.015	0.031	0.062	0.123	0.246	0.492	0.985	1.969
Note	Input Wave : Sign wave(0.005Hz) - 3Cycles / Step Average Shear Strain = (Lamina No.13 displacement) / (Ground Height)							

3 TEST RESULTS AND DISCUSSIONS

3.1 Bending moment and Axial force by centrifuge acceleration

Figure 4 shows the distributions of the bending moment at the centrifugal acceleration of 50G. The bending moments and axial forces were calculated from the measured strains of the tunnel using the equation below. The results were discussed in full-scale values, i.e. prototype values.

$$M = - \frac{(\epsilon_{out} - \epsilon_{in}) \times E \times t^2}{12 \times (1 - \nu^2)} \quad (1)$$

$$N = \frac{(\epsilon_{out} + \epsilon_{in}) \times E \times t}{2 \times (1 - \nu^2)} \quad (2)$$

where M : bending moment

N : axial force

ϵ_{out} : strain at the outside of tunnel lining

ϵ_{in} : strain at the inside of tunnel lining

E : elastic modulus of tunnel

t : thickness of tunnel lining

ν : poisson's ratio of tunnel

The maximum bending moment of circular and rectangular tunnels is almost the same value of 20kNm/m. The distributions show the following tendencies; i) in the case of circular tunnels, the bending moment becomes large at the spring-line and the upper/lower parts. The moment of rectangular tunnels, on the other hand, seems to be raised from the top and bottom slabs to each corner and at the connections of a center column. ii) moment values and the distributions of triple-faced tunnel are approximately the same as the single tunnels.

Axial force becomes large at sides of lining in both type of tunnels and center columns in rectangular tunnel. Its maximum value is about 180kN/m.

It can be thought that the shear box except loading apparatus will deform slightly during increasing centrifugal acceleration. The sectional force, therefore, does not distribute symmetrically. In the subsequent section on cyclic loading tests, the test results are discussed using incremental sectional force aiming at removing the effects of the shear box deformation before cyclic loading.

3.2 Bending moment and Axial force by cyclic loading

3.2.1 Behavior of active type shear box

In order to verify the fundamental cyclic properties of the shear box and the ground displacement at

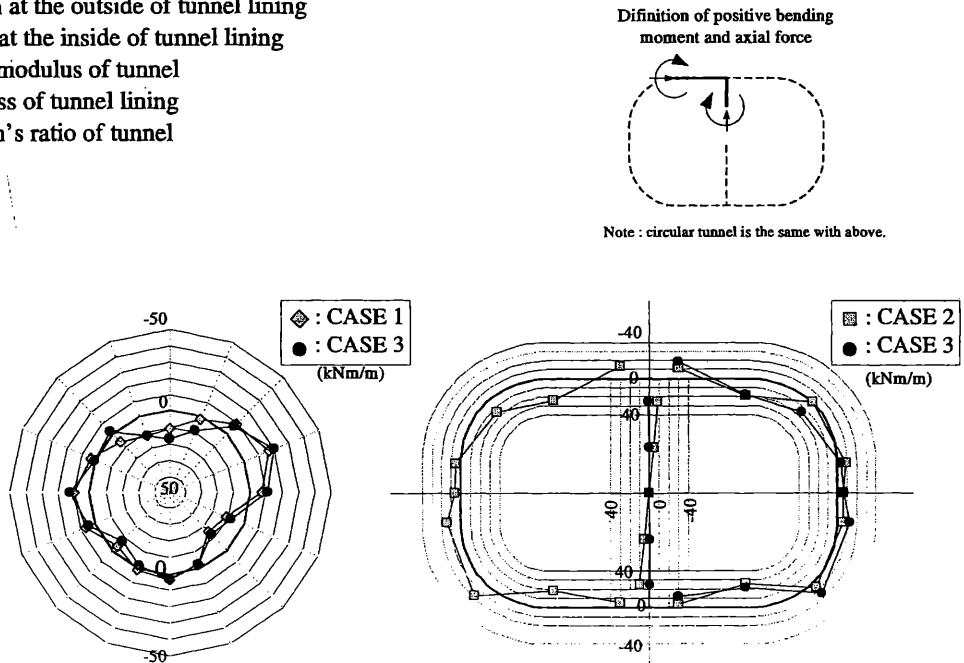


Figure 4. Bending moment at the centrifugal acceleration 50G (: initial).

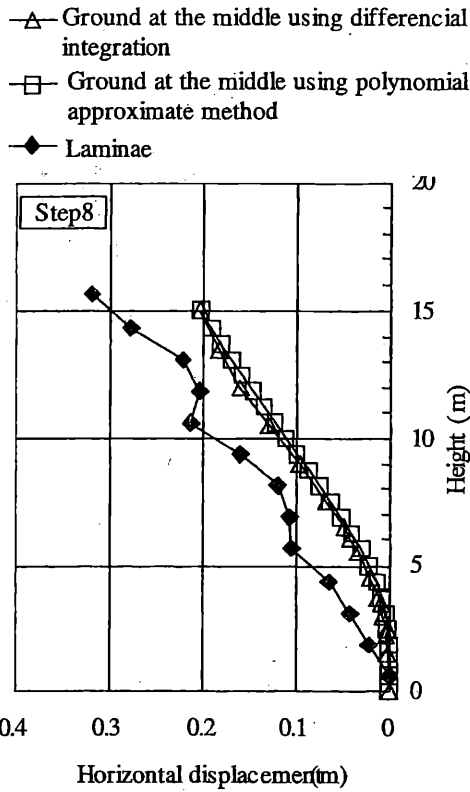


Figure 5. Displacement of laminae and ground

the middle, a loading test of sand without tunnels was performed in the same way as the tests mentioned in Section 2. Figure 5 represents the displacement of each lamina at one quarter of a loading cycle for step 8. The Figure also shows the ground displacement at the middle calculated by applying integration methods in the depth direction using the surface displacement and strain behaviors of a phosphorous bronze plate (thickness: 0.2 mm, width: 5mm). As shown in the Figure, the displacement of the ground at the middle generally coincides with the simple shear mode and is about 70% of given displacement.

3.2.2 Behaviors of the single circular tunnel and rectangular tunnel with center columns

Figure 6 shows the sectional forces, bending moment and axial force of both single circular and rectangular tunnels caused by cyclic shear for the first cycle of each loading step. Here the sectional forces for a center column of the rectangular tunnel are values for the unit length along the longitudinal direction of tunnel, taking into consideration the intervals of the columns.

The findings are summarized as follows; 1) Sectional forces at the corners are remarkable. 2) Bending moment is also large at ends of a center column.

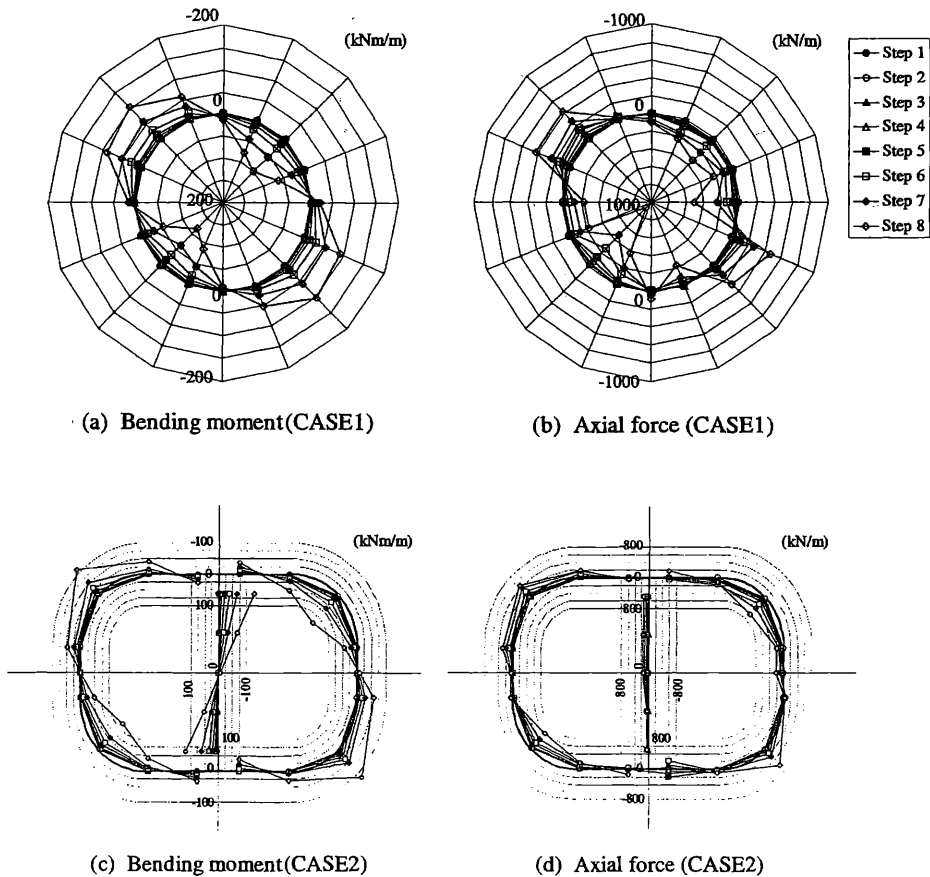


Figure 6. Behavior of single tunnels

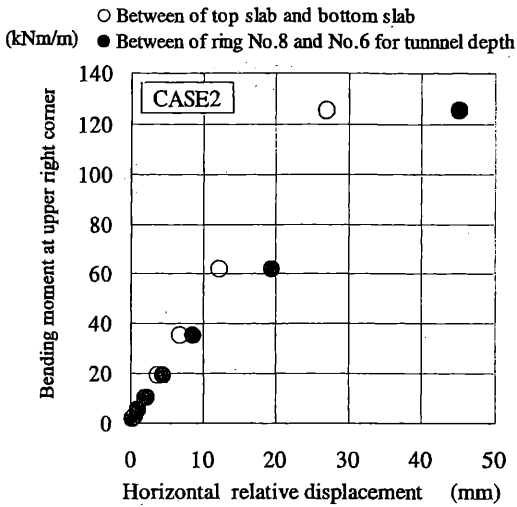


Figure 7. Relationship between bending moment and horizontal relative displacement

3) The distribution of sectional forces seems to be the same irrespective of loading steps. 4) The maximum values of bending moment and axial force are 110kNm/m and 600kN/m, respectively. Both of them become larger than those before cyclic loading.

Figure 7 shows the bending moments and relative displacements between two laminae (i.e. R6 and R8 on figure 2) located at tunnel's elevation for the single rectangular tunnel. The relation of bending moments and horizontal relative displacements between the top and bottom slabs is also shown in the Figure. The former displacements can be regarded as ground displacements. As shown in the Figure, these relations will be different tendency. The bending moment will not be proportional to the laminae relative displacements, whereas it will be almost in proportion to relative displacements between two slabs of the tunnel. It seems to indicate that relative displacement of tunnel and ground takes place and it is important to evaluate tunnel's displacement.

Table 2. Horizontal relative displacements for rectangular tunnels.

	(mm)							
Step	1	2	3	4	5	6	7	8
CASE2 (Single tunnel)	0.25	0.56	1.00	2.03	3.81	6.90	12.37	27.00
CASE3 (Triple-faced tunnel)	0.15	0.31	0.53	1.14	2.31	4.78	8.80	16.50

3.2.3 Behavior of triple-faced tunnel

The comparison of the distribution of the bending moments at step8 for the triple-faced tunnel and that for the single circular and rectangular tunnels is shown in Figure 8. This Figure shows that there is not much difference between the triple-faced tunnel and single tunnel in circular cases, though the depths of each tunnel differ. Meanwhile, in case of the rectangular tunnel of triple-faced tunnel, bending moments reduce compared with single case despite the same difference in depths as circular tunnels. Horizontal relative displacement between the top and bottom slabs for the triple-faced rectangular tunnel is smaller of 1.65cm than that of 2.7cm for single-faced tunnel at step 8. The tendency is the same for all the steps shown in table 2.

Figure 9 shows the bending moments compared with triple-faced and single-faced rectangular tunnel at almost the same displacements. For example, the displacement at step2 in case2 is almost the same with the one at step3 in case3, and so on. The bending moment at the lower right corner in triple-faced tunnel, that is adjacent to circular tunnel, seems to become greater larger than that in single tunnel at almost the same displacement.

As mentioned above, concerning the horizontal relative displacement and distribution of bending moment, the mechanical behavior of triple-faced tunnel is different from the single tunnel. The former

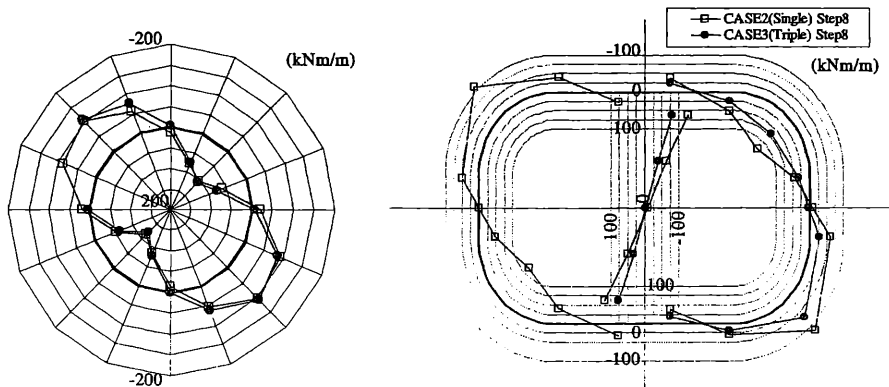


Figure 8. Comparison between single tunnel and triple-faced tunnel (bending moment).

will globally influence on bending moment of tunnel. On the other hand, the later will locally influence on it. It will be important to pay attention to these effects for the design of a multi-faced adjacent tunnel.

4 CONCLUSION

Centrifuge model tests were performed to understand the response of a circular tunnel, a rectangular tunnel with center columns, and a combination of these two (triple-faced tunnel consisting of two circular tunnels and a rectangular tunnel) subjected to cyclic large shear deformation. The test results exhibited the same tendency as the findings from previous studies: the increase of the sectional forces (bending moment and axial force) due to cyclic shear deformation was large at 45 degrees from spring-line/corners, and at the top and bottom ends for the center columns. The mechanical behavior of triple-faced tunnel is different from the single tunnel concerning the horizontal relative displacement of tunnel and distribution of bending moment and it will be important to pay attention to these effects.

Based on the test results represented in this paper, the future studies will establish a method for evaluating the behaviors of large cross-section tunnels and complex cross-section tunnels during large earthquakes.

ACKNOWLEDGEMENTS

The authors are most grateful for advice given by Dr. O. Kusakabe, Professor of the Tokyo Institute of Technology.

REFERENCES

- Japanese association for the sewers and sewage. 1997. Guideline for countermeasures of sewers and sewage against earthquake (in Japanese)
- Public Works Research Institute et al. 1989. Comprehensive research report on the development of the design technique for underground structures against earthquake. Comprehensive research report. Vol29. Public Works Research Institute (in Japanese)

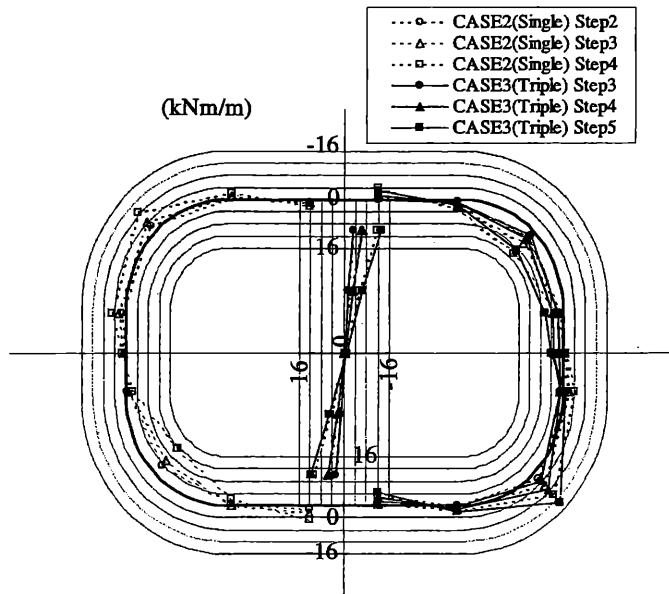


Figure 9. Comparison between single tunnel and triple-faced tunnel (bending moment) for approximately same displacement.